

# Radiative Effects on Boundary-Layer Flow of a Nanofluid on a Continuously Moving or Fixed Permeable Surface

Ali J. Chamkha<sup>a</sup>, Mohamed Modather<sup>b,c</sup>, Saber M.M. EL-Kabeir<sup>b,c</sup> and Ahmed M. Rashad<sup>\*b</sup>

<sup>a</sup>Manufacturing Engineering Department, The Public Authority for Applied, Education and Training, Shuweikh 70654, Kuwait; <sup>b</sup>Department of Mathematics, Aswan University, Faculty of science, Egypt; <sup>c</sup>Department of Mathematics, Salman Bin Abdul Aziz University, College of Science and Humanity Studies, Al-Kharj, KSA

Received: May 16, 2012; Accepted: July 16, 2012; Revised: July 20, 2012

**Abstract:** In recent years, significant patents have been devoted to developing nanotechnology in industry since materials with sizes of nanometers possess unique physical and chemical properties. Due to recent advances in nanotechnology, a new class of heat transfer fluids called nanofluids was discovered. A nanofluid is a mixture produced by dispersing metallic nanoparticles in low thermal conductivity liquids such as water, oils, lubricants and others to enhance the heat transfer performance. Many patents have been devoted to the methods of preparation of new nanofluids heat transfer. Nanofluids are now being developed for medical applications, including cancer therapy and safer surgery by cooling. In this paper, a study of a boundary layer flow and heat transfer characteristics of an incompressible nanofluid flowing over a permeable uniform heat flux surface moving continuously in the presence of radiation is reported. The Rosseland diffusion approximation is used to describe the radiative heat flux in the energy equation. The resulting system of non-linear ordinary differential equations are solved numerically using a finite difference method. Numerical results are obtained for the velocity, temperature and nanoparticles volume fraction profiles, as well as the friction factor, local Nusselt number and local Sherwood number for several values of the parameters, namely the velocity ratio parameter, suction/injection parameter, Brownian motion parameter, thermophoresis parameter and radiation parameter. It is found that an increase in either of the Brownian motion parameter or the thermophoresis parameter leads to reductions in the local Nusselt number and the local Sherwood number. In addition, increasing either of the suction/injection parameter or the radiation parameter causes enhancements in both the local Nusselt number and the local Sherwood number.

**Keywords:** Moving surface, nanofluid, radiation effect, suction/injection.

## 1. INTRODUCTION

The study of convective heat transfer of nanofluids is gaining a lot of attention. Nanofluids have many applications in the industries since materials of nanometer size have unique physical and chemical properties. Nanofluids are solid-liquid composite materials consisting of solid nanoparticles or nanofibers with sizes typically of 1-100nm suspended in liquid. Recently, nanofluids have attracted a great interest because of reports of significant enhancement in their thermal properties. For example, a small amount (< 1% volume fraction) of Cu nanoparticles or carbon nanotubes dispersed in ethylene glycol or oil is reported to increase the inherently poor thermal conductivity of the liquid by 40% and 150%, respectively [1, 2]. Conventional particle-liquid suspensions require high concentration (>10%) of particles to achieve such enhancement. However, problems of rheology and stability are amplified at high concentration, precluding the widespread use of conventional slurries as heat transfer fluids. In some cases, the observed enhancement in thermal conductivity of nanofluids is orders of magnitude larger than predicted by well-established theories. Other perplexing results in this rapidly evolving field include a

surprisingly strong temperature dependence of the thermal conductivity [3] and a three-fold higher critical heat flux compared with the base fluids [4, 5]. These enhanced thermal properties are not merely of academic interest. If confirmed and found consistent, they would make nanofluids promising for application in thermal management. Furthermore, suspensions of metal nanoparticles are also being developed for other purposes, such as medical applications including cancer therapy. The interdisciplinary nature of nanofluid research presents a great opportunity for exploration and discovery at the frontiers of nanotechnology. Kuznetsov and Nield [6] have also studied the classical problem of free convection boundary layer flow of a viscous and incompressible fluid (Newtonian fluid) past a vertical flat plate to the case of nanofluids. Khan and Pop [7] analyzed the development of the steady boundary layer flow, heat transfer and nanoparticle fraction over a stretching surface in a nanofluid.

Bachok *et al.* [8] have investigated the steady boundary-layer flow of a nanofluid past a moving semi-infinite flat plate in a uniform free Stream. Syakila and Pop [9] studied the steady mixed convection boundary layer flow past a vertical flat plate embedded in a porous medium filled with nanofluids using different types of nanoparticles.

Application of nanofluids for heat transfer enhancement of separated flows encountered in a backward facing step

\*Address correspondence to this author at the Department of Mathematics, Aswan University, Faculty of Science, Egypt; Tel: +2010147647047; Fax: +20973480450; E-mail: am\_rashad@yahoo.com

presented by Abu-Nada [10]. Duangthongsuk and Wongwises [11] analyzed the effect of thermophysical properties models on the predicting of the convective heat transfer coefficient for low concentration nanofluid. A similarity analysis for the problem of a steady boundary-layer flow of a nanofluid on an isothermal stretching circular cylindrical surface is presented by Gorla *et al.* [12]. Gorla *et al.* [13] have also studied mixed convective boundary layer flow over a vertical wedge embedded in a porous medium saturated with a nanofluid. Noghrehabadi *et al.* [14] studied effect of partial slip boundary condition on the flow and heat transfer of nanofluids past a stretching sheet with prescribed constant wall temperature.

The characteristics of flow and heat transfer of a viscous and incompressible fluid over flexed or continuously moving flat surfaces in a moving or a quiescent fluid are well understood. These flows occur in many manufacturing processes in modern industry, such as hot rolling, hot extrusion, wire drawing and continuous casting. For example, in many metallurgical processes such as drawing of continuous filaments through quiescent fluids and annealing and tinning of copper wires, the properties of the end product depends greatly on the rare of cooling involved in these processes. Sakiadis [15] was the first one to analyze the boundary layer flow on continuous surfaces. Crane [16] obtained an exact solution the boundary layer flow of Newtonian fluid caused by the stretching of an elastic sheet moving in its own plane linearly. El-Kabeir [17] studied the interaction of forced convection and thermal radiation during the flow of a surface moving continuously in a flowing stream of micropolar fluid with variable viscosity. El-Kabeir *et al.* [18] discussed a similarity analysis for the problem of the steady boundary-layer flow of a micropolar fluid on a continuous moving permeable surface with uniform heat flux.

One of the first related patents regarding the development of nanofluids was that by Choi and Eastman [19] who invented an apparatus and method for enhancing the heat transfer in liquids namely, water, ethylene glycol and oil. The method involves dispersing nanoparticles of copper, copper oxide and aluminum oxide in these liquids. Li *et al.* [20] invented a one-step method for preparing nanofluids consisting of metal oxide nanoparticles dispersed in oily fluids such as lubricant oils. A more recent related patent is that of Zhang and Lockwood [21] on enhancing the thermal conductivity of fluids using high thermal conductivity graphite nanoparticles and carbon nanotubes. Lockwood *et al.* [22] invented a method for gear oil composition containing nanoparticles. Hajikata *et al.* [23] invented a heat transport nanofluid important for heat exchanger thermal energy transfer. This nanofluid includes a solvent, surface-coated particles together with organic components dispersed in the solvent. Hong and Wensel [24] invented a nanofluid that contains carbon nanoparticles, metal oxide nanoparticles and a surfactant in a thermal transfer fluid. Their invention relates to processes for producing such a nanofluid with enhanced thermal conductive properties. Hayes and McCants [25] recently invented a nanofluid for thermal management systems in which they used a base liquid with zinc oxide nanoparticles at a concentration of of about 0.01% to about 5% by volume. Cardenas *et al.* [26] invented special nanofluids and methods of use for drilling and completion fluids. These flu-

ids containing nanomaterials, such as carbon nanotubes, meet the required rheological and filtration properties for application in challenging HPHT drilling and completions operations.

We present here a similarity analysis for the problem of steady boundary-layer flow of a nanofluid on a continuous moving permeable uniform heat flux surface in the presence of the radiation effect. The development of the velocity, temperature and nanoparticles volume fraction profiles distributions have been illustrated for several values of nanofluid parameters, velocity ratio, suction/injection parameters and radiation parameter.

## 2. ANALYSIS

Consider a flat surface moving at a constant velocity  $u_w$  in a parallel direction to a free stream of a nanofluid of uniform velocity  $u_\infty$ . Either the surface velocity or the free-stream velocity may be zero but not both at the same time. The physical properties of the fluid are assumed to be constant. Under such condition, the governing equations of the steady, laminar boundary-layer flow on the moving surface are given by (see, El-Kabeir *et al.* [18]):

$$\frac{\partial u}{\partial x} + \frac{\partial v}{\partial y} = 0 \tag{1}$$

$$u \frac{\partial u}{\partial x} + v \frac{\partial u}{\partial y} = \nu \frac{\partial^2 u}{\partial y^2} \tag{2}$$

$$u \frac{\partial T}{\partial x} + v \frac{\partial T}{\partial y} = \alpha \frac{\partial^2 T}{\partial y^2} - \frac{1}{\rho C_p} \frac{\partial q_r}{\partial y} + \tau D_B \frac{\partial T}{\partial y} \frac{\partial C}{\partial y} + \frac{\tau D_T}{T_\infty} \left(\frac{\partial T}{\partial y}\right)^2 \tag{3}$$

$$u \frac{\partial C}{\partial x} + v \frac{\partial C}{\partial y} = D_B \frac{\partial^2 C}{\partial y^2} + \frac{D_T}{T_\infty} \frac{\partial^2 T}{\partial y^2} \tag{4}$$

In the above equations,  $u$ ,  $v$ ,  $T$  and  $C$  are the  $x$ - and  $y$ -components of fluid velocity, temperature and nanoparticles volume fraction, respectively.  $\alpha$ ,  $\rho$ ,  $\tau$ ,  $q_r$ ,  $D_B$  and  $D_T$  are the thermal diffusivity, density of ambient fluid, nanofluid heat capacity ratio, heat flux in the  $y$ -direction, Brownian diffusion coefficient, and the thermophoretic diffusion coefficient, respectively.

The corresponding initial and boundary conditions for this problem can be written as:

$$u = \pm u_w, v = v_w, \frac{\partial T}{\partial y} = -\frac{q_w}{k}, \frac{\partial C}{\partial y} = -\frac{m_w}{D_B}, \text{ at } y = 0, \tag{5}$$

$$u \rightarrow u_\infty, T \rightarrow T_\infty, C \rightarrow C_\infty \text{ as } y \rightarrow \infty$$

The boundary condition of  $u = u_w$  in (5) represents the case of a plane surface moving in parallel to the free stream and  $q_w$  and  $m_w$  represent the wall heat and mass fluxes, respectively.

To analyze the effect of both the moving and the free stream on the boundary-layer flow, we propose a new similarity coordinate and a dimensionless stream function

$$\eta = \frac{y}{x} (\text{Re}_w + \text{Re}_\infty)^{1/2}, f = \frac{\psi}{\nu (\text{Re}_w + \text{Re}_\infty)^{1/2}} \tag{6}$$

which are the combinations of the traditional ones:

$$f_B = \frac{\Psi}{\nu \text{Re}_\infty^{1/2}}, \quad \eta_B = \frac{y}{x} \text{Re}_\infty^{1/2} \quad (7)$$

for the Blasius problem (stationary wall and uniform free stream velocity) and

$$f_s = \frac{\Psi}{\nu \text{Re}_w^{1/2}}, \quad \eta_s = \frac{y}{x} \text{Re}_w^{1/2} \quad (8)$$

from the Sakiadis (uniformly moving wall with stagnant free stream) problem. The Reynolds numbers are defined as:

$$\text{Re}_w = \frac{u_w x}{\nu}, \quad \text{Re}_\infty = \frac{u_\infty x}{\nu} \quad (9)$$

A velocity ratio parameter  $\gamma$  is defined as

$$\gamma = \frac{u_w}{u_w + u_\infty} = (1 + \frac{u_\infty}{u_w})^{-1} = (1 + \frac{\text{Re}_\infty}{\text{Re}_w})^{-1} \quad (10)$$

Note that from the Blasius problem  $u_w = 0$ , therefore  $\gamma = 0$ .

On the other hand, for the Sakiadis problem  $u_\infty = 0$  and thus  $\gamma = 1$ . In addition, we also define dimensionless temperature and concentration function as

$$\theta = \frac{T - T_\infty}{q_w x / (\text{Re}_w + \text{Re}_\infty)^{1/2}}, \quad \phi = \frac{C - C_\infty}{m_w x / (\text{Re}_w + \text{Re}_\infty)^{1/2}} \quad (11)$$

and the radiation

$$q_r = -\frac{4\sigma^* \partial T^4}{3k^* \partial y}$$

$$T^4 = T_\infty^4 + 4T_\infty^3(T - T_\infty) + 6T_\infty^2(T - T_\infty)^2 + \dots$$

$$\cong -3T_\infty^4 + 4T_\infty^3 T \quad (12)$$

$$\frac{\partial q_r}{\partial y} = -\frac{16T_\infty^3 \sigma^* \partial^2 T}{3k^* \partial y^2}$$

Using the transformation variables defined in equations (6-12), the governing transformed equations may be written as:

$$f''' + \frac{1}{2} f f'' = 0 \quad (13)$$

$$\frac{1}{\text{Pr}} (1 + \frac{4}{3} R_d) \theta'' + \frac{1}{2} f \theta' + \text{Nb} \theta' \phi' + \text{Nt} \theta'^2 = 0 \quad (14)$$

$$\frac{1}{\text{Le}} \phi'' + \frac{1}{\text{Le}} \frac{\text{Nt}}{\text{Nb}} \theta'' + \frac{1}{2} f \phi' = 0 \quad (15)$$

The transformed initial and boundary conditions become:

$$f(0) = f_w, f'(0) = \pm \gamma, \theta'(0) = -1, \phi'(0) = -1,$$

$$f'(\infty) = 1 - \gamma, \theta(\infty) = \phi(\infty) = 0 \quad (16)$$

where Eq. (1) is identically satisfied. In Eqs. (13-16), a prime indicates differentiation with respect to  $\eta$  and the parameters

$$\text{Nt} = \frac{\tau D_T q_w (\text{Re}_w + \text{Re}_\infty)^{1/2}}{T_\infty (u_w + u_\infty)}, \text{Nb} = \frac{\tau D_B m_w (\text{Re}_w + \text{Re}_\infty)^{1/2}}{(u_w + u_\infty)},$$

$$R_d = \frac{4\sigma^* T_\infty^3}{k^* k}, \text{Pr} = \frac{\nu}{\alpha}, \text{Le} = \frac{\nu}{D}, f_w = -\nu_w \frac{2(\text{Re}_w + \text{Re}_\infty)^{1/2}}{(u_w + u_\infty)} \quad (17)$$

Here,  $\text{Pr}, R_d, f_w, \text{Le}, \text{Nb}$  and  $\text{Nt}$  denote the Prandtl number, the radiation parameter, suction/injection parameter, the Lewis number, the Brownian motion parameter and the thermophoresis parameter respectively. It is important to note that this boundary value problem reduces to the classical problem of flow and heat and mass transfer due to a the Blasius problem when  $\text{Nb}$  and  $\text{Nt}$  are zero. Most nanofluids examined to date have large values for the Lewis number  $\text{Le} > 1$  (see Nield and Kuznetsov [27]). For water nanofluids at room temperature with nanoparticles of 1-100 nm diameters, the Brownian diffusion coefficient  $D_B$  ranges from  $4 \times 10^{-4}$  to  $4 \times 10^{-12} \text{ m}^2/\text{s}$ . Furthermore, the ratio of the Brownian diffusivity coefficient to the thermophoresis coefficient for particles with diameters of 1-100 nm can be varied in the ranges of 2-0.02 for alumina, and from 2 to 20 for copper nanoparticles (see Buongiorno [28] for details). Hence, the variation of the non-dimensional parameters of nanofluids in the present study is considered to vary in the mentioned range.

Of special significance for this type of flow and heat transfer situation are the local skin-friction coefficient, local Nusselt number and the local Sherwood number. These physical parameters can be defined in dimensionless form as:

$$Cf_\infty \text{Re}_\infty^{1/2} = 2(1 - \gamma)^{-3/2} |f''(0)|, \quad (18)$$

$$Cf_w \text{Re}_w^{1/2} = 2\gamma^{-3/2} |f''(0)|$$

$$\text{Nu}_x / \text{Re}_\infty^{1/2} = \frac{(1 + \frac{4}{3} R_d)}{\theta(0)} \quad (19)$$

$$\text{Sh}_x / \text{Re}_\infty^{1/2} = \frac{1}{\phi(0)} \quad (20)$$

### 3. RESULTS AND DISCUSSIONS

In order to get a clear insight of the physical problem, numerical results are displayed with the help of graphical and tabulated illustrations. The system of equations (13-15) with the boundary conditions (16) were solved numerically by means of an efficient, iterative, tri-diagonal implicit finite-difference method discussed previously by Blottner [29]. Since the changes in the dependent variables are large in the immediate vicinity of the plate while these changes decrease greatly as the distance away from the plate increases, variable step sizes in the  $\eta$  direction were used. The used initial step size in the  $\eta$  direction was  $\Delta\eta_1 = 0.001$  and the growth factor was  $K_\eta = 1.0375$  such that  $\Delta\eta_n = K_\eta \Delta\eta_{n-1}$ . This indicated that the edge of the boundary layer  $\eta_\infty = 35$ . The convergence criterion used was based on the relative difference between the current and the previous iterations which was set to  $10^{-5}$  in the present work. It is possible to compare the results obtained by this numerical method with the previously published work of El-Kabeir *et al.* [18]. Table 1 shows that excellent agreement between the results exists. This lends confidence in the numerical results to be reported subsequently. Computations were carried out for various values of parameters at  $\text{Pr} = 0.7$  and  $\text{Le} = 10$ . The results of this parametric study are shown in Figs. (2-15).

**Table 1. Comparison of Skin Friction  $f''(0)$  for Various Values of Velocity Ratio  $\gamma$ .**

| $\gamma$ | EL-Kabeir <i>et al.</i> [18] | Present Results |
|----------|------------------------------|-----------------|
| 0.0      | 0.3321                       | 0.3323          |
| 0.1      | 0.2783                       | 0.2784          |
| 0.2      | 0.2173                       | 0.2174          |
| 0.3      | 0.1501                       | 0.1501          |
| 0.4      | 0.0775                       | 0.0773          |
| 0.5      | 0                            | 0               |
| 0.6      | -0.0819                      | -0.0820         |
| 0.7      | -0.1677                      | -0.1678         |
| 0.8      | -0.2570                      | -0.2569         |
| 0.9      | -0.3494                      | -0.3495         |
| 1.0      | -0.4445                      | -0.4440         |

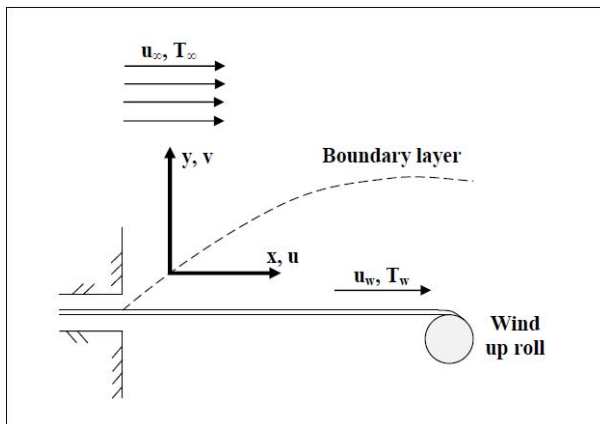


**Fig. (1).** Physical model and coordinates system.

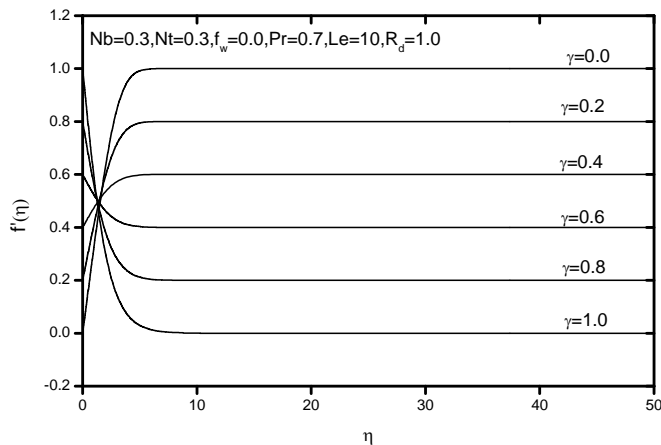


**Fig. (2).** Velocity profiles with various values of velocity ratio parameter  $\gamma$ .

Figures 2-4 display the effect of velocity ratio  $\gamma$  on the velocity, temperature and volume fraction profiles, respectively. It can be seen that, the velocity of the fluid increases as velocity ratio  $\gamma$  increases in cases  $\gamma < 0.5$  and decreases in case  $\gamma > 0.5$ , on the other hand the temperature  $\theta$  of the fluid increases as velocity ratio  $\gamma$  increases, while nanoparticle volume fraction  $\phi$  decreases as velocity ratio  $\gamma$  increases.

Figures 5 & 6 present the effect of thermophoresis parameter  $N_t$  and Brownian motion parameter  $N_b$  on the temperature  $\theta$  and nano-particle volume fraction  $\phi$ , respectively. It can be seen that, temperature  $\theta$  and nanoparticle volume fraction  $\phi$  of the fluid increase as thermophoresis parameter  $N_t$  and Brownian motion parameter  $N_b$  increase.

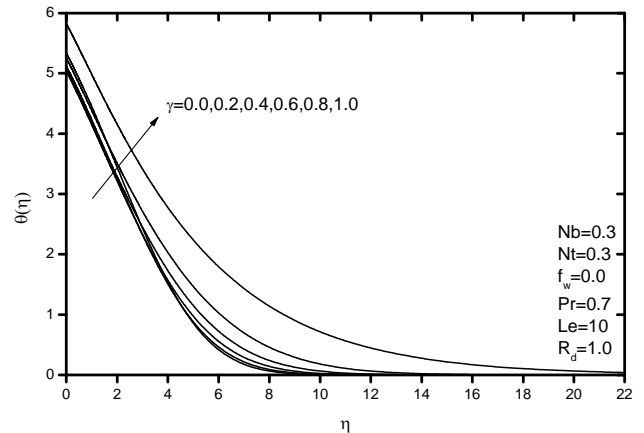


**Fig. (3).** Temperature profiles with various values of velocity ratio parameter  $\gamma$ .

Figures 7 & 8 display the effect of thermophoresis parameter  $N_t$  and Brownian motion parameter  $N_b$  on local Nusselt number and local Sherwood number respectively. It can be seen that the thermophoresis parameter  $N_t$  appears in the

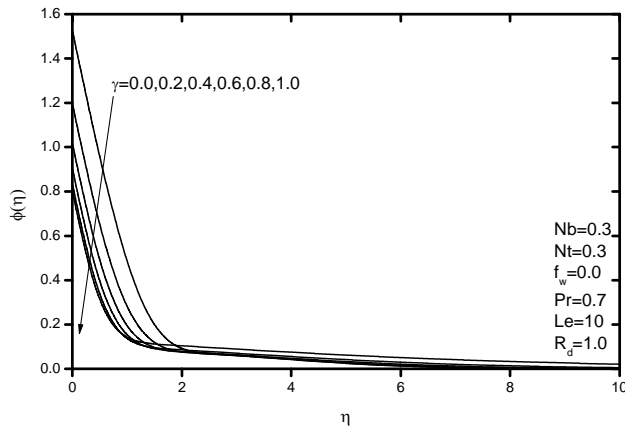


Fig. (4). Volume fraction profiles with various values of velocity ratio parameter  $\gamma$ .

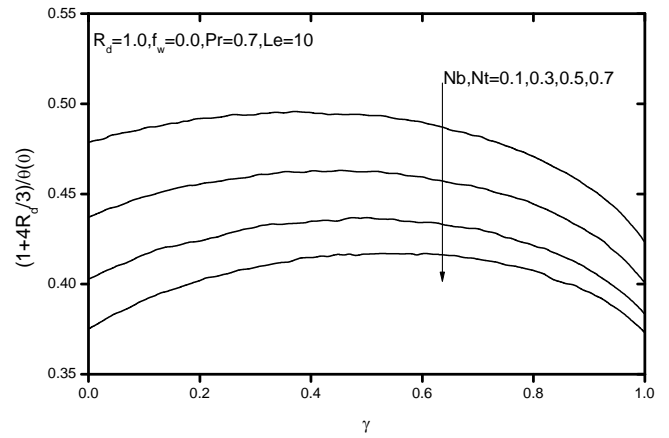


Fig. (7). Local Nusselt number with various values of  $Nb$  and  $Nt$ .

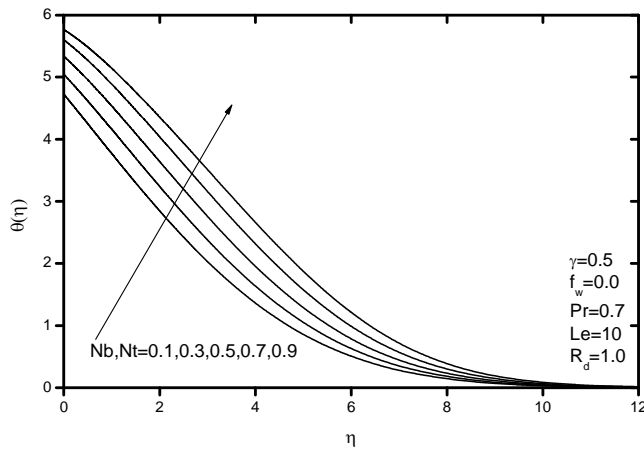


Fig. (5). Temperature profiles with various values of  $Nb$  and  $Nt$ .

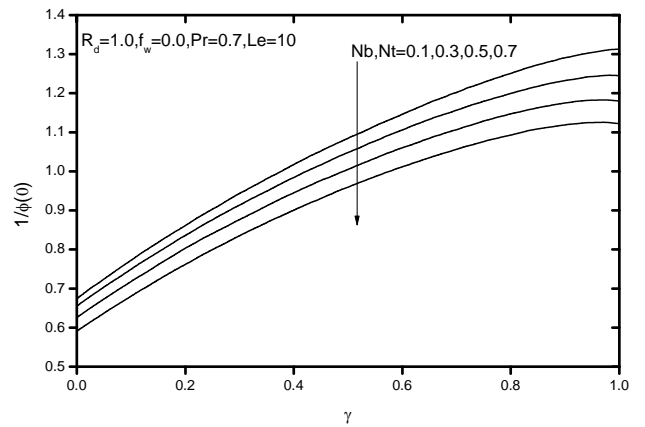


Fig. (8). Local Sherwood number with various values of  $Nb$  and  $Nt$ .

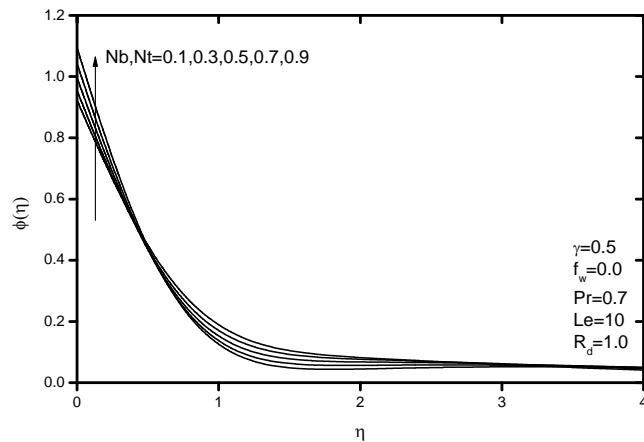


Fig. (6). Volume fraction profiles with various values of  $Nb$  and  $Nt$ .

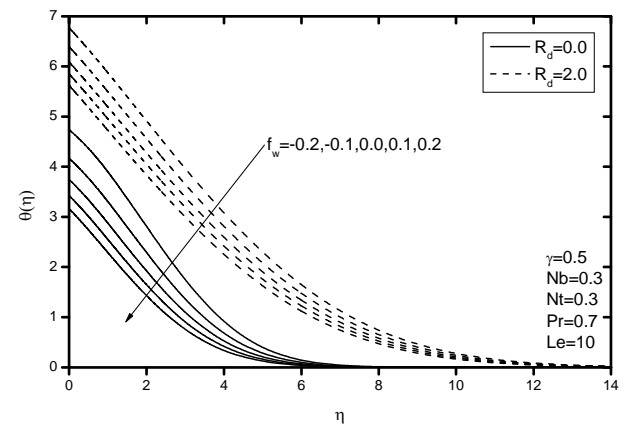


Fig. (9). Temperature profiles with various values of  $f_w$  and  $R_d$ .

thermal and concentration boundary layer equations. As we note, it is coupled with the temperature function and plays a strong role in determining the diffusion of heat and nanoparticles concentration in the boundary layer. Moreover, In nanofluid systems, owing to the size of the nanoparticles,

Brownian motion takes place, and this can enhance the heat transfer properties. This is due to the fact that the Brownian diffusion promotes heat conduction. The nanoparticles increase the surface area for heat transfer. A nanofluid is a two phase fluid where the nanoparticles move randomly and increase the energy exchange rates. However, the Brownian motion reduces nanoparticles diffusion. The increase in the

local Sherwood number as  $Nb$  changes is relatively small. Therefore, as indicated before, increasing the Brownian motion parameter  $N_b$  and the thermophoresis parameter  $N_t$  cause increasing the temperature and volume fraction profiles. This yields reduction in the local Nusselt number and local Sherwood number.

Figures 9 & 10 show the representative of temperature and nanoparticles volume fraction profiles for different values of suction/injection  $f_w$  and radiation  $R$  parameters, respectively. It can be observed that the increasing the value of suction/injection parameter  $f_w$  causes decreasing in both temperature and volume fraction profiles, while radiation  $R$  leads to a significant change in temperature and slight change in volume fraction, as radiation parameter increases the temperature of the fluid increases and volume fraction decreases.

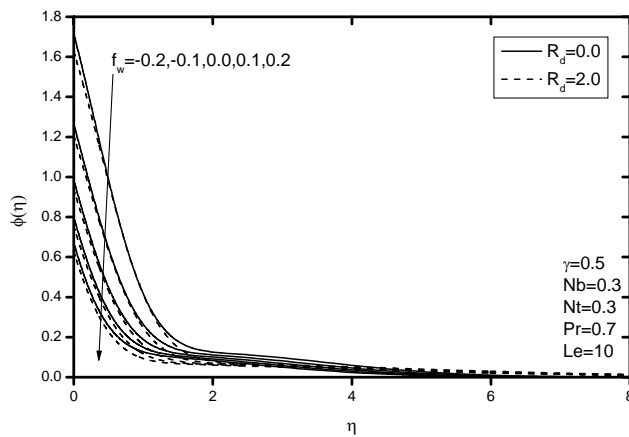


Fig. (10). Volume fraction profiles with various values of  $f_w$  and  $R_d$ .

Figure 11 displays the effect of velocity ratio  $\gamma$  and suction/injection  $f_w$  parameters on the values of local skin friction coefficient, It can be seen that, local skin friction decreases as velocity ratio  $\gamma$  increases in cases  $\gamma < 0.5$  and increases in case  $\gamma > 0.5$ , while local skin friction coefficient increases as suction/injection  $f_w$  parameter increases.

Finally, Figs. (12-15) show the effect of suction/injection  $f_w$  and radiation parameters on local Nusselt number and local Sherwood number, respectively. It can be seen that increasing the value of suction/injection  $f_w$  and radiation parameters led to increasing in both local Nusselt number and local Sherwood number.

4. CURRENT & FUTURE DEVELOPMENTS

The objective of the present work was to study the effect of thermal radiation on boundary layer flow of an incompressible nanofluid flowing over a permeable uniform heat flux surface moving continuously. Some related patents for the preparation of heat transfer nanofluids are highlighted. The model used for the nanofluid incorporated the effects of Brownian motion and thermophoresis. The governing boundary layer equations were solved numerically using an efficient, implicit finite-difference method. The local skin-friction coefficient, local Nusselt number and the local

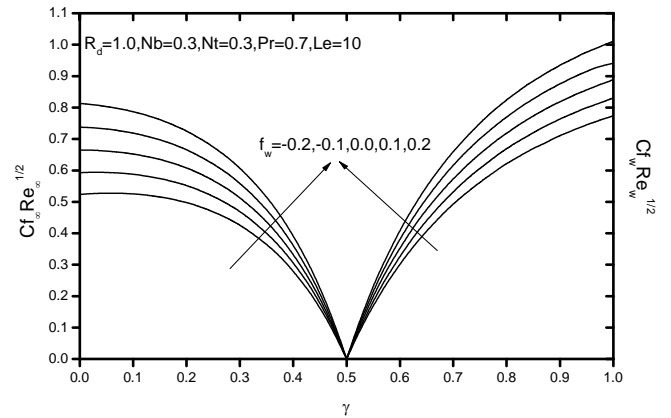


Fig. (11). Local skin-friction coefficient with various values of  $f_w$ .

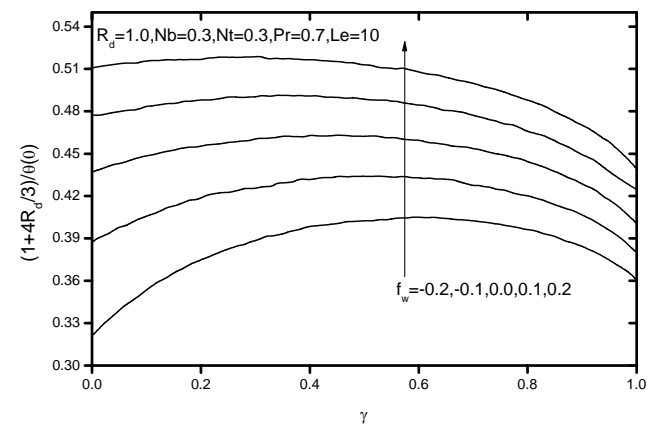


Fig. (12). Local Nusselt number with various values of  $f_w$ .

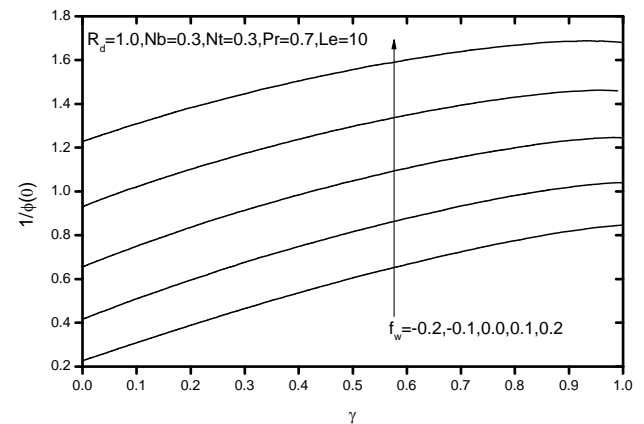


Fig. (13). Local Sherwood number with various values of  $f_w$ .

Sherwood number as well as the temperature, concentration and velocity distributions for various values of the velocity ratio, suction/injection parameter, radiation parameter and nanofluid parameters were illustrated graphically and discussed. Based on the obtained results of the above numerical investigation, the following conclusions could be drawn:

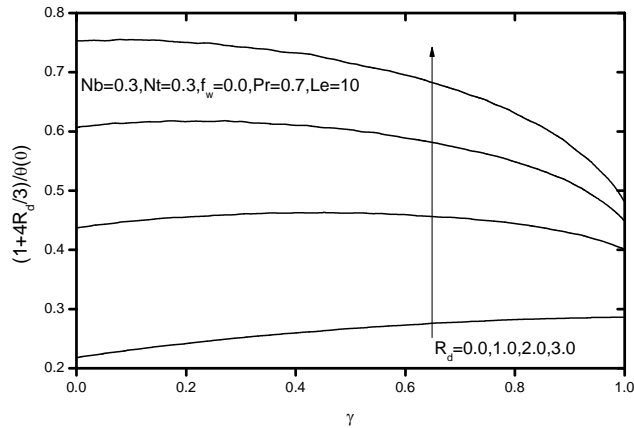


Fig. (14). Local Nusselt number with various values of  $R_d$ .

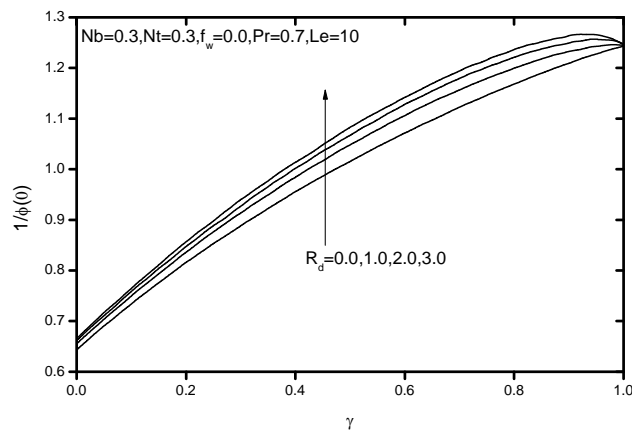


Fig. (15). Local Sherwood number with various values of  $R_d$ .

- 1- It was found that both of the temperature of the fluid and the nanoparticles volume fraction increase as either of the thermophoresis parameter or the Brownian motion parameter increased.
- 2- Increasing the suction/injection parameter caused reductions in both the temperature and nanoparticles volume fraction profiles. On the other hand, increasing the thermal radiation parameter led to a significant change in temperature and a slight change in the nanoparticles volume fraction.
- 3- The fluid temperature increased while the nanoparticles volume fraction decreased as the velocity ratio increased.
- 4- Increases in either of the Brownian motion parameter or the thermophoresis parameter led to reductions in the local Nusselt and Sherwood numbers.
- 5- As either of the suction/injection parameter or the radiation parameter increased, both the local Nusselt number and the local Sherwood number enhanced.

### CONFLICT OF INTEREST

The authors confirm that this article content has no conflicts of interest.

### ACKNOWLEDGEMENTS

The authors are thankful to the reviewers for their positive comments and their valuable suggestions which led to definite improvements in the paper.

### REFERENCES

- [1] Eastman JA, Choi SUS, Li S, Yu W, Thompson LJ. Anomalous increased effective thermal conductivities containing copper nanoparticles. *Appl Phys Lett* 2001; 78: 718-20.
- [2] Choi SUS, Zhang ZG, Yu W, Lockwood FE, Grulke EA. Anomalous thermal conductivity enhancement on nanotube suspensions. *Appl Phys Lett* 2001; 79: 2252-4.
- [3] Patel HE, Das SK, Sundararajan T, Sreekumaran A, George B, Pradeep T. Thermal conductivities of naked and monolayer protected metal nanoparticle based nanofluids manifestation of anomalous enhancement and chemical effects. *Appl Phys Lett* 2003; 83: 2931-3.
- [4] You SM, Kim JH, Kim KH. Effect of nanoparticles on critical heat flux of water in pool boiling heat transfer. *Appl Phys Lett* 2003; 83: 3374-6.
- [5] Vassallo P, Kumar R, D'Amico S. Pool boiling heat transfer experiments in silica water nonfluids. *Int J Heat Mass Transfer* 2004; 47: 407-11.
- [6] Kuznetsov AV, Nield DA. Natural convective boundary-layer flow of a nanofluid past a vertical plate. *Int J Therm Sci* 2010; 49: 243-7.
- [7] Khan WA, Pop I. Boundary layer flow of nanofluid past a stretching sheet. *Int J Heat Mass Transfer* 2010; 53: 2477-83.
- [8] Bachok N, Ishak A, Pop I. Boundary layer flow of nanofluid over moving surface in a flowing fluid. *Int J Therm Sci* 2010; 49: 1663-8.
- [9] Syakila A, Pop I. Mixed convection boundary layer flow from a vertical flat plate embedded in a porous medium filled with nanofluids. *Int Comm Heat Mass Transfer* 2010; 37: 987-91.
- [10] Abu-Nada E. Application of nanofluids for heat transfer enhancement of separated flows encountered in a backward facing step. *Int J Heat Fluid Flow* 2008; 29: 242-9.
- [11] Duangthongsuk W, Wongwises S. Effect of thermophysical properties models on the predicting of the convective heat transfer coefficient for low concentration nanofluid. *Int Comm Heat Mass Transfer* 2008; 35: 1320-6.
- [12] Gorla RSR, EL-Kabeir SMM, Rashad AM. Boundary-layer heat transfer from a stretching circular cylinder in a nanofluid. *J Thermophys Heat Transfer* 2011; 25(1): 183-6.
- [13] Gorla RSR, Chamkha AJ, Rashad AM. Mixed convective boundary layer flow over a vertical wedge embedded in a porous medium saturated with a nanofluid: Natural convection dominated regime. *Nanoscale Res Lett* 2011; 6: 1-9.
- [14] Noghrehabadi A, Pourrajab R, Ghalambaz M. Effect of partial slip boundary condition on the flow and heat transfer of nanofluids past stretching sheet prescribed constant wall temperature. *Int J Therm Sciences* 2012; 54:253-261.
- [15] Sakiadis BC. Boundary-layer behavior on a continuous solid surface: II-The boundary layer on a continuous flat surface. *AIChE J* 1961; 7: 221-5.
- [16] Crane LJ. Flow past a stretching plate. *ZAMP* 1970; 21: 645-7.
- [17] EL-Kabeir SMM. Radiative effects on forced convection flows in micropolar fluids with variable viscosity. *Can J Phys* 2004; 82: 151-65.
- [18] EL-Kabeir SMM, Rashad AM, Gorla RSR. Heat transfer in a micropolar fluid flow past a permeable continuous moving surface. *ZAMM* 2011; 92(5): 360-70.
- [19] Choi, S.U.S., Eastman, J.A. Enhanced heat transfer using nanofluids. *US6221275 (2001)*.
- [20] Li C, Young M, Shih R, Wen M, Chang M. Process for preparing nanofluids with rotating packed bed reactor. *TW263675 (2006)*.
- [21] Zhang, Z., Lockwood, F.E. Enhancing thermal conductivity of fluids with graphite nanoparticles and carbon nanotube. *US7348298 (2008)*.
- [22] Lockwood, F.E., Zhang, Z., Wu, G., Smith, T.R. Gear oil composition containing nanomaterial. *US20080242566 (2008)*.

- [23] Hijikata, Y., Torigo, E., Kawaguchi, T., Morishita, T. Heat transport fluid, heat transport structure, and heat transport method. US20080054217 (**2008**).
- [24] Hong, H., Wensel, J. Carbon nanoparticle-containing hydrophilic nanofluid with enhanced thermal conductivity. US20118075799 (**2011**).
- [25] Hayes, A.M., McCants, D.A. Nanofluids for thermal management systems. US20120006509 (**2012**).
- [26] Quintero, L., Cardenas, A.E., Clark, D.E. Nanofluids and methods of use for drilling and completion fluids. US20120015852 (**2012**).
- [27] Nield DA, Kuznetsov AV. Thermal instability in a porous medium layer saturated by a nanofluid. *Int J Heat Mass Transfer* 2009; 52: 5796-801.
- [28] Buongiorno J. Convective transport in nanofluids. *J Heat Trans-T, ASME* 2006;128: 241-50.
- [29] Blottner FG. Finite-difference methods of solution of the boundary-layer equations. *AIAA J* 1970; 8: 193-205.